

Additional Mission Applications for NASA's 13.3-kW Ion Propulsion System

John Steven Snyder
Jet Propulsion Laboratory
California Institute of Technology
4800 Oak Grove Dr.
Pasadena, CA 91109
818-393-7357
Steve.Snyder@jpl.nasa.gov

David Manzella
NASA Glenn Research Center
21000 Brookpark Road
Cleveland, OH 44135
216-977-7432
David.Manzella@nasa.gov

Doug Lisman
Jet Propulsion Laboratory
California Institute of Technology
4800 Oak Grove Dr.
Pasadena, CA 91109
818-354-9295
P.D.Lisman@jpl.nasa.gov

Robert E. Lock
Jet Propulsion Laboratory
California Institute of Technology
4800 Oak Grove Dr.
Pasadena, CA 91109
818-393-2525
Robert.E.Lock@jpl.nasa.gov

Austin Nicholas
Jet Propulsion Laboratory
California Institute of Technology
4800 Oak Grove Dr.
Pasadena, CA 91109
818-354-4206
Austin.K.Nicholas@jpl.nasa.gov

Ryan Woolley
Jet Propulsion Laboratory
California Institute of Technology
4800 Oak Grove Dr.
Pasadena, CA 91109
818-393-8279
Ryan.C.Woolley@jpl.nasa.gov

Abstract— NASA's Space Technology Mission Directorate has been recently developing critical technologies for high-power solar electric propulsion (SEP), including large deployable solar array structures and high-power electric propulsion components. An ion propulsion system based on these developments has been considered for many SEP technology demonstration missions, including the Asteroid Redirect Robotic Mission (ARRM) concept. These studies and the high-power SEP technology developments have generated excitement within NASA about the use of the ARRM ion propulsion system design for other types of potential missions. One application of interest is for Mars missions, especially with the types of orbiters now under consideration for flights in the early 2020's to replace the aging Mars Reconnaissance Orbiter. High-power SEP can deliver large payloads to Mars with many additional capabilities, including large orbital plane changes and round-trip missions, compared to chemically-propelled spacecraft. Another application for high-power SEP is for exo-planet observation missions, where a large starshade spacecraft would need to be repositioned with respect to its companion telescope relatively frequently and rapidly. SEP is an enabling technology for the ambitious science goals of these types of missions. This paper will discuss the benefits of high-power SEP for these concepts based on the STMD technologies now under development.

from the laboratory to operational status while directly contributing to the present-day widespread use of SEP for North-South station keeping on hundreds of commercial telecommunication satellites.¹ Over the same time period, NASA SEP applications have been limited to the kilowatt-class Dawn and Deep Space-1 missions. As interest in higher-power missions has grown, the NASA Space Technology Mission Directorate (STMD) in 2010 began the developments necessary to enable SEP systems at power levels up to 50 kW in a way that would also have extensibility to next-generation systems at power levels in excess of 200 kW. These developments have focused on large deployable solar array structures and high-power electric propulsion components with a range of cross-cutting applications. The accomplishments in each of these technology areas are summarized below.

In April of 2012 NASA released a solicitation for the development of the technology needed for mass and volume efficient, large-area solar array systems (SAS) with total power levels of 30-50 kW with extensibility to power levels of 250 kW or greater for previously identified high power SEP cargo applications.² Mass and stowed volume efficiency were specifically targeted for advancements relative to state-of-art systems because improvements in these area will enable high power SEP vehicles to fit within the lift capability and fairing constraints of current launch vehicles such as the family of Evolved Expendable Launch Vehicles (EELVs) including the Atlas V and the Delta IV. In August 2012 NASA STMD selected two companies for SAS development efforts: Deployable Space Systems (DSS) of Goleta, California and ATK Space Systems Inc., of Commerce, California.³ In 2014, under contract to NASA Glenn Research Center, each of these contracted efforts demonstrated engineering development unit (EDU) 20-kW-class solar array wings. These demonstrations resulted in advanced solar arrays for SEP applications up to 50 with a technology readiness level of at least five.

TABLE OF CONTENTS

1. INTRODUCTION.....	1
2. MARS ORBITER MISSIONS	3
3. STARSHADE EXOPLANET MISSIONS.....	7
4. SUMMARY	11
ACKNOWLEDGEMENTS	11
REFERENCES.....	12
BIOGRAPHY	12

1. INTRODUCTION

The investments NASA has made in solar electric propulsion (SEP) over the last fifty years have matured this technology

Deployable Space System (DSS) designed, manufactured, and tested an EDU Roll Out Solar Array (ROSA) wing 6.2-meters wide and 13.6-meters long that was sized to produce approximately 20 kW. ROSA employs a pair of composite booms that serve as both the primary structure for the wing and the deployment actuator. The use of the composite booms provides a level of strength and stiffness approximately an order of magnitude greater than state-of-art rigid solar arrays. The photovoltaic blanket consists of standard solar cells bonded to a flexible substrate that is rolled onto a mandrel in the stowed configuration.

ATK Space Systems designed, manufactured and tested a 9.7-meter diameter EDU MegaFlex solar array wing sized to provide approximately 17 kW. MegaFlex is an evolution of ATK's heritage UltraFlex solar array that was successfully flown on the NASA Mars Phoenix lander and has been flight qualified for Orbital Sciences Corporation's Cygnus commercial resupply spacecraft. Megaflex improves upon the fan-fold, tensioned membrane design of UltraFlex by introducing an additional hinge in the radial structural elements to further reduce the size of the stowed solar array wing. Megaflex employs a photovoltaic blanket consisting of individual triangular gores supported by radial composite spars. The individual gores consist of conventional solar cells bonded to a flexible substrate that fold in half in the stowed configuration. The circular design of the MegaFlex is particularly attractive to high power SEP applications because of the low moment of inertia associated with this geometric configuration.

In the Fall of 2011, while planning the SAS procurement, STMD made the decision to focus technology development efforts addressing Hall thruster and power processing unit (PPU) technology to be compatible with the solar arrays then slated for development. This was done in order to enable a 30-50 kW SEP transportation capability with the type of crosscutting applicability that has been desired for decades. The thruster technology development was based on recent advancements in long-life Hall thrusters utilizing the concept of magnetic shielding as previously demonstrated with 5-kW class thrusters.^{4,5,6} The objective was to develop a 15-kW class Hall thruster incorporating these innovations to a technology readiness level of five. A design point corresponding to 12.5 kW of input power, 3000 seconds of specific impulse, and an operational lifetime of up to 50,000 hours were targeted, as was the ability to throttle to lower powers and lower specific impulses. An initial technology demonstration unit (TDU) thruster, shown in Fig. 1, was designed, fabricated, and experimentally evaluated.⁷ The thruster was operated over discharge voltages of 300V to 800 V and discharge powers of 0.6 kW to 12.5 kW, generating up to 680 mN of thrust, with a peak specific impulse of 3,000 sec and peak efficiency of 63%.⁸

The PPU employs a modular design with full-bridge topology.^{9,10} Four 3.5-kW discharge modules can be configured in different stacked architectures or individually disabled to provide a range of output voltages and currents at

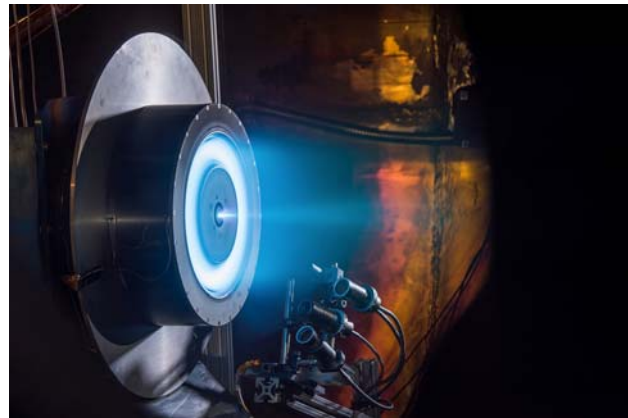


Fig. 1. TDU Thruster in Performance Test.

high efficiency. The input voltage range of 95V to 140V can accommodate a wide variety of missions. A development unit PPU has demonstrated total efficiencies as high as 95% in benchtop testing and has been operated successfully with the TDU thruster.

The further development of the STMD thruster and PPU to flight-qualified status with an industrial partner is ongoing. The technical characteristics of the desired electric propulsion string comprised of the PPU, thruster, and low-pressure xenon flow controller (XFC) are described in detail in the NASA solicitation for this co-development.¹¹ The solicitation calls for a throttleable 12.5-kW xenon thruster, a PPU that controls the thruster and XFC outputs and operations as well as hosts a command and control interface with the spacecraft. Each string is sized for a nominal 13.3 kW input power, accounting for the PPU efficiency and the total power required by the thruster and XFC.

The performance requirements for the EP string are shown in Table 1.¹¹ The thruster life requirement is for a total impulse of 10^8 Newton-seconds, with a maximum mass of 43 kg. The PPU operates with a high-voltage bus input voltage of 95 V to 140 V and has a maximum mass of 42 kg. The XFC independently controls the xenon flow rate to the cathode and anode for inlet pressures between 344-689 kilopascals (50-100 psia) and has a maximum mass of 2.5 kg. Additional EP string characteristics are listed in the Component End-Item Requirements Section of the referenced solicitation. Note that the system power throttling range for this solicitation is focused toward missions within the heliocentric range of Mars, but the hardware itself is capable of a much greater throttling range as demonstrated by recent test results.⁸

NASA is currently planning to conduct the in-space flight demonstration of this newly developed SEP technology as part of the proposed Asteroid Redirect Robotic Mission (ARRM).¹² ARRM seeks to demonstrate the advanced SEP technologies needed to support future human-crewed missions to Mars by performing a robotic mission to collect a multi-ton asteroid mass from the surface of a large near Earth asteroid (NEA). This mission would also include the demonstration of a planetary defense technique called an

Table 1. Minimum EP String Performance Requirements.*

EP String Total Input Power (kW)	Discharge Voltage (V)	Thrust (mN)	Mass Flow Rate (mg/s)	System Efficiency
13.33	400	686	30.66	0.58
13.33	600	589	22.91	0.57
13.33	700	553	20.36	0.56
13.33	800	526	18.52	0.56
10.00	300	562	29.69	0.53
10.00	400	521	24.30	0.56
10.00	500	482	20.89	0.56
10.00	600	446	18.31	0.54
10.00	700	413	16.17	0.53
10.00	800	342	12.88	0.45
6.67	300	386	21.65	0.52
6.67	400	342	17.55	0.50
6.67	500	311	14.83	0.49
6.67	600	267	11.43	0.47
6.67	700	242	9.99	0.44

* Performance requirements include measurement uncertainties. See Ref. 9 for details.

enhanced gravity tractor prior to returning the Asteroid Redirect Vehicle (ARV) and asteroid mass to a crew-accessible, stable orbit around the Moon. Astronauts onboard the NASA Orion spacecraft would then explore the returned asteroid mass in the mid 2020's in what is being called the Asteroid Redirect Crewed Mission (ARCM). An illustration of the ARV acquiring an asteroid mass from the surface of a large NEA is shown in Fig. 2. ARRM utilizes 40 kW of power for SEP, processed by three 13.3-kW strings (an additional string is included as a spare). Further details on the ARRM IPS, including system architecture, can be found elsewhere.⁹



Fig. 2. Asteroid Redirect Robotic Mission Concept.

While this SEP technology development activity is currently geared toward ARRM, its capabilities have generated significant interest within other communities within NASA. This paper will present and describe two very different applications of the ARRM system: a Mars orbiter mission and a trio of telescope-starshade missions. For convenience, the STMD-developed electric propulsion hardware will be referred to here as the ARRM ion propulsion system.

2. MARS ORBITER MISSIONS

Mission Motivation and Goals

NASA is exploring concepts for science and telecommunications orbiters for launch to Mars in 2022 or 2024. One of the motivating factors of these studies is the need to replenish reconnaissance and telecommunications relay functions currently provided by aging spacecraft at Mars. Other factors include advancing potential sample return goals and extending science investigations to include new questions uncovered by recent orbiter and rover discoveries and the need to find key resources to support future Mars human and robotic missions

Both chemical and SEP propulsion options are under consideration for these studies. Compared to previous chemical propulsion Mars missions such as MRO, SEP would enable orbiters to have several additional capabilities while also fitting in the lowest cost of the expendable launch vehicle range such as Atlas V-401 and Falcon 9. These include:

- Dramatically Improved ΔV Capability
 - Round Trip Mission – returning the orbiter (and some payload) back to Earth
 - Large plane or altitude changes in Mars orbit
- Improved Payload Accommodation
 - Larger payload mass allocation
 - Excess solar power available for instruments or communications
 - “Daughtercraft” payloads
- More Flexible Operations
 - Wide launch periods in any year (several months)
 - Spiral trajectories that have natural close flybys of Phobos and Deimos
 - No critical events – orbit insertion and aerobraking risks are eliminated

SEP does have some disadvantages, chiefly a somewhat longer flight time when maximizing delivered mass (2 – 2.5 years to Low Mars Orbit instead of 1.5 years).

Several of the many options under study for the next Mars orbiter are designed to use the high power electric propulsion components under development by STMD for missions such as the proposed ARRM. The high power ion propulsion system and large deployable solar array structures have significant potential to enable mission options far exceeding those of previous Mars missions.

To provide an example of these improvements, one option currently under study will be examined here in more detail. This option is designed to meet a variety of mission goals and takes specific advantage of the added capabilities provided by potential ARRM solar electric propulsion components. We present an example set of mission goals, trajectory, and orbiter system configuration to illustrate just one of many options. All options have significant trades in play for varying objectives, capabilities, and margins.

Potential mission objectives of a 2022 Mars orbiter include:

- Replenishment of the relay telecommunications and high resolution reconnaissance observations established by the Mars Reconnaissance Orbiter mission in 2006
- Demonstration of progress in Mars orbit towards potential sample return
- Accommodation of new science investigations
 - Searching for shallow ground ice
 - Finding and linking possible brine flows with ground ice and atmospheric conditions
 - Characterization of dynamic atmospheric processes
 - Characterization of mineral composition in a variety of settings
- Finding resources on Mars in support of human exploration and other future missions
 - Find and quantify shallow ground ice and its overburden
 - Find deposits of hydrated minerals
 - Identify site-specific mineral resources and geotechnical properties
- Validate high power SEP use in a Mars mission context
- Develop experience operating deep space optical communication (DSOC) at Mars

Trajectory Design for Mars Sample Return

In this paper we will examine a case study for a Mars Sample Return Mission using components of the ARRM Ion Propulsion System. For a typical Mars orbiter, SEP can provide a significant mass savings compared to a bipropellant mission. The use of SEP really shines, however, in the high ΔV requirements of a sample return orbiter. Previous concepts¹³ for Mars Sample Return have used chemical propulsion, which led to very large launch masses and extreme sensitivity to additional mission ΔV . A SEP thruster such as the one discussed in this paper has a specific impulse that is 5-10 times that of chemical thrusters. This reduces fuel

mass requirements significantly, which more than offsets the mass required for additional power.

The low thrust and long thrusting times of SEP missions create a whole spectrum of possible trajectories to and from Mars, in contrast to the discrete trajectories of ballistic missions. Whereas ballistic trajectories are largely independent to mission specifics, SEP trajectories are dependent on thrust, mass, power, flight times, launch vehicle, etc. It is important to simultaneously optimize the trajectory, propulsion system, and spacecraft parameters to fully utilize SEP’s capabilities. For missions to Mars it is recommended to have a nominal acceleration of 0.1-0.2 mm/s² at Earth. One ARRM engine could push a spacecraft in the 2500 – 4000 kg range, which is the high end of the Falcon 9 launch vehicle’s performance capabilities for interplanetary launches. In this application, having a high specific impulse will maximize the mass delivered to Mars, with the optimum falling between 4000 and 5000 seconds.¹⁴ The ARRM engine is capable of specific impulses of 3000 seconds, which is extremely high for a Hall thruster, and results in significant propellant savings.

For this case study we used a single EP string with a redundant spare string, i.e. a 1+1 propulsion system. Other mission assumptions are listed in Table 2. The power was selected to maximize useful payload (see Figure 4) and is not sufficient to fully power the ion propulsion system (IPS) at Mars distances. A PPU capable of throttling down to as little as 4 kW was assumed. The IPS is operated at full power near Earth and switches to lower throttle settings as it moves further away from the sun. Only “direct” trajectories were considered, meaning direct launch to Earth escape without the aid of Earth spirals or gravity assists.

Table 2. Mission Design Assumptions for a Mars Sample Return Orbiter.

Parameter	Assumption
Earth Launch Year	2022
Launch Vehicle	Falcon 9 v1.1
Earth Arrival Year	2031
Mars Orbit	320 km x 75°
Nominal Power	27 kW

In order to optimize the mission concept, thousands of trajectories were simulated while parametrically varying parameters such as flight times, spacecraft mass, and power levels and compiled into a database for use in spacecraft sizing studies. This was done for both the outbound and inbound portions of the mission. Some of the results are illustrated in Fig. 3. From the left figure (Earth to Mars), it can be seen that the mass delivered to Low Mars Orbit (LMO) increases with both power and time of flight, but with a diminishing return on both. The right figure shows a similar trend for the Mars to Earth transfer. It clearly shows that for each power level, there is a clear “knee” in the curve (red star

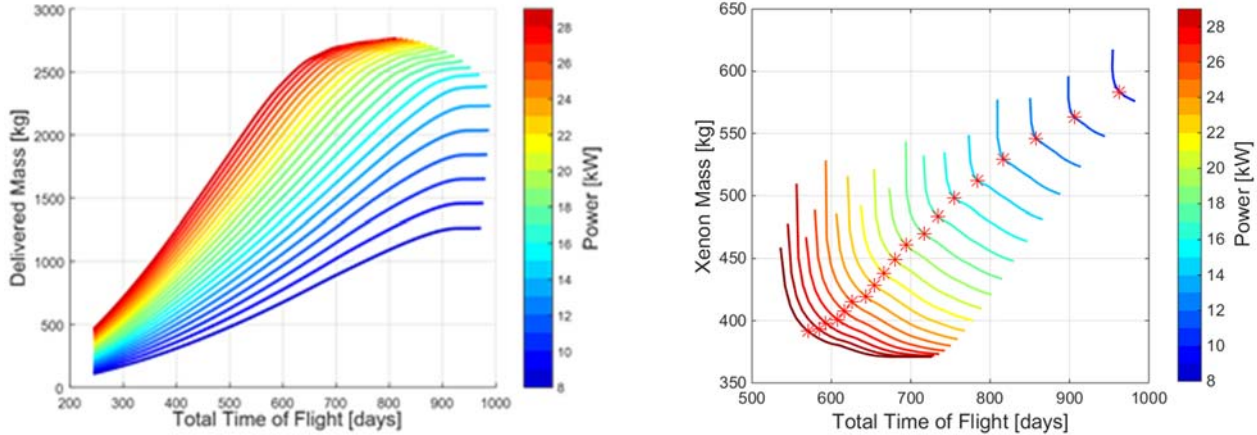


Fig. 3. Left: Earth-to-Mars Trajectory Family - Mass delivered to Low Mars Orbit (320 km altitude) as a function of total time-of-flight and power. Right: Mars-to-Earth Trajectory Family - Total xenon mass required to deliver 1500 kg to a 1.5 km/s Earth intercept from Low Mars Orbit.

markers) where further increasing time of flight only marginally improves performance. However, neither of these plots accounts for the fact that increasing the power causes more of the delivered mass to be consumed by the power system. This will be discussed in the next section.

By sweeping through launch and arrival dates for our selected parameters is possible to create a mission design tool called a Bacon plot, which similar to a ballistic porkchop plot. Analysis of these Bacon plots show that it is possible to create a continuous or nearly continuous launch period if one is willing to accept trip times above 2.5 years. It also shows that Earth arrival will optimally occur in the fall of 2031 with a Mars departure on any date in 2029 or early 2030.¹⁵

Fig. 4 and Fig. 5 show the optimized trajectories for this mission. Launch takes place in July of 2022 to a low C3 of $3.4 \text{ km}^2/\text{s}^2$. Following a 30-day forced coast checkout period,

thrusting begins and continues for nearly the entire 473-day trip to Mars encounter. The thrust direction is indicated by the red arrows. Upon arrival at Mars the spacecraft then spirals down to low Mars orbit over the next 300 days to arrive in August 2024. After 5 years at Mars and collecting the orbiting sample, the spacecraft then spirals out and begins a 1.6 year transfer back to Earth. Nearly half of the return trajectory is spent coasting. The spacecraft arrives in 2033 with a V_∞ of 1.5 km/s, which allows for a direct capture to a stable lunar orbit.

In addition to maneuvers required to get the spacecraft from Earth to Mars and back again, a few other maneuvers would be required or desired in Mars orbit. The largest of these maneuvers is a 15° inclination change to shift from a 75° orbit to a 90° orbit. This plane change would allow global science observations with rotating time-of-day (from 75°), and polar

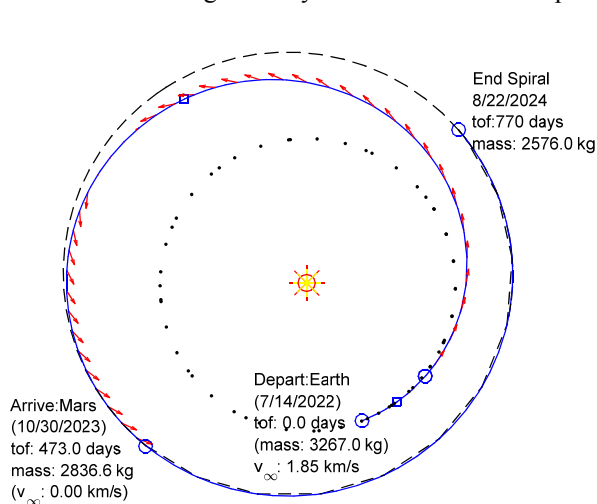


Fig. 4. Earth-to-Mars Transfer. Includes a 30-day checkout after launch and a 300-day spiral at Mars down to a 320 km orbit.

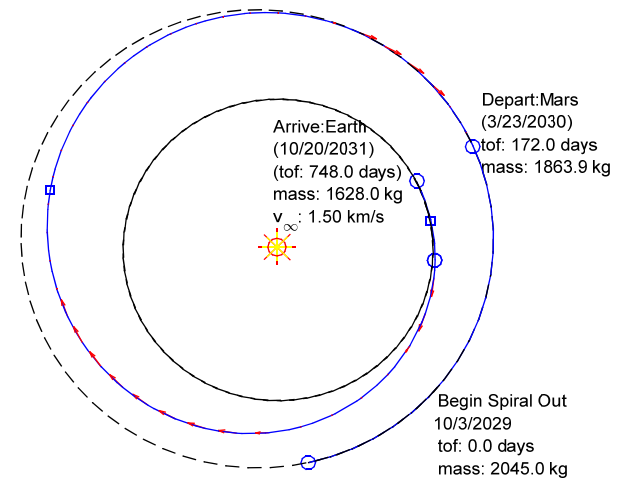


Fig. 5. Mars-to-Earth Transfer. Includes a spiral-out from 320 km and a forced 30-day coast before arrival. End condition is $V_{inf} = 1.5 \text{ km/s}$ which facilitates capture to Lunar Distant Retrograde Orbit (DRO).

observations and fixed time-of-day observations globally (from $\sim 90^\circ$). In many ways, this is like a second science mission, as it allows fundamentally different science questions to be addressed for almost no incremental cost. The propellant budget also includes an allocation for matching orbits (“rendezvous”) with a potential orbiting sample container.

Table 3 shows the notional delta V budget and timeline for this notional mission. The total delta V to be performed by the SEP system is 15.6 km/s, of which roughly 50% is maneuvers at Mars and 50% is the cruises from Earth to Mars and back again. The inbound and outbound cruise phases each take approximately 2.1 years, and approximately 5 years are spent at Mars. Of these 5 years at Mars, approximately 4 of them are dedicated to science, and the remaining year involves maneuvering for the plane change or rendezvous maneuvers (some science can still be performed during these maneuvers).

Table 3. Notional ΔV Budget and Timeline for Mars Sample Return.

	ΔV [km/s]	Duration [years]	Start Date
Earth-to-Mars Cruise	4.0	1.3	Jul-2022
Spiral to LMO	2.6	0.8	Oct-2023
Corrections	0.1		
15° Plane Change	1.4	5.1	Aug-2024
Sample Rendezvous	0.3		
Spiral from LMO	3.0	0.5	Oct-2029
Mars-to-Earth Cruise	4.2	1.6	Mar-2030
Total	15.6	9.3	End Date Oct-2031

Spacecraft Design

For the purpose of this study, “payload mass” is the figure of merit we seek to optimize. As defined here, “payload mass” could be three things: 1) sample capture and return hardware, or 2) science instruments, or 3) carried daughtercraft. This figure of merit is a proxy for the science return of the mission. It is worth noting that a very capable ~ 200 kg telecom subsystem is assumed in order to provide a robust relay and optical communication infrastructure, and this is not counted as “payload”. For a rough sense of scale, the science payload of MRO was 140 kg and the sample capture and return hardware is estimated to have a mass of 120 kg.

Having defined notional mission goals and explored the trajectory, it is then necessary to build a spacecraft which accomplishes those goals while following a feasible trajectory. Using a parametric/interpolation-based modeling approach, all spacecraft subsystem masses are sized iteratively until the spacecraft size matches feasible inbound and outbound trajectories, and the payload mass is maximized within feasibility constraints. The model estimates reflect significant margins in mass (30% of total

system dry mass), solar array power capacity (15% above end-of-life power), and propellants (10%). These margins in a SEP mission can be used interchangeably and residual margins at launch can be used in flight to improve mission performance through shorter mission phase durations or additional ΔV .

An example of a parametric sweep across spacecraft power is shown in Fig. 6. The whole spacecraft and associated trajectory are re-sized for each power level. The optimal power level (maximizing payload at 270 kg) is approximately 27 kW in this case. As power levels increase from 15-25 kW, it can be seen that the trajectory is improving because more launch mass is used (which means that the launch vehicle is launching to a lower C3 and taking greater advantage of SEP). As power increases beyond 30kW, the extra mass of additional solar panels outweighs the trajectory benefits that the additional power provides, causing a decrease in payload capability.

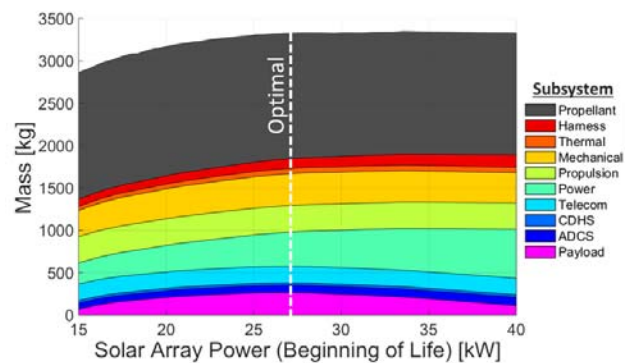


Fig. 6. Notional spacecraft subsystem mass breakdown as a function of solar array power. The power level resulting in optimal payload capability is marked with the vertical white line.

The optimal vehicle has an overall mass of approximately 3300 kg, and propellant mass fraction of 43%. While this seems very heavy for a Mars mission (MRO was ~ 2200 kg), recall that it launches to a very low C3 (~ 3 km²/s²), which means it would still fit on an Atlas V 401 or Falcon 9 class vehicle. This low mass fraction for a round trip mission highlights the advantages of using SEP for this application.

A chemical orbiter for sample return was previously studied.¹⁶ In comparison, this multi-function SEP orbiter fares very favorably. The chemical orbiter did not have any science payload, had a less capable telecom system, and did not do any large plane changes. Even lacking all of these features, it still had a launch mass of 3300 kg and a propellant mass fraction of 70% using 325s bipropellant propulsion. Its trajectory requires a launch energy of C3=12 km²/s². This means that it would require an Atlas V-531 class launch vehicle. For a *very rough* estimate at equivalent comparison, adding the extra features present in the SEP concept to the chemical orbiter would increase its dry mass by at least 30% (for the extra science instruments, telecom gear, and structure

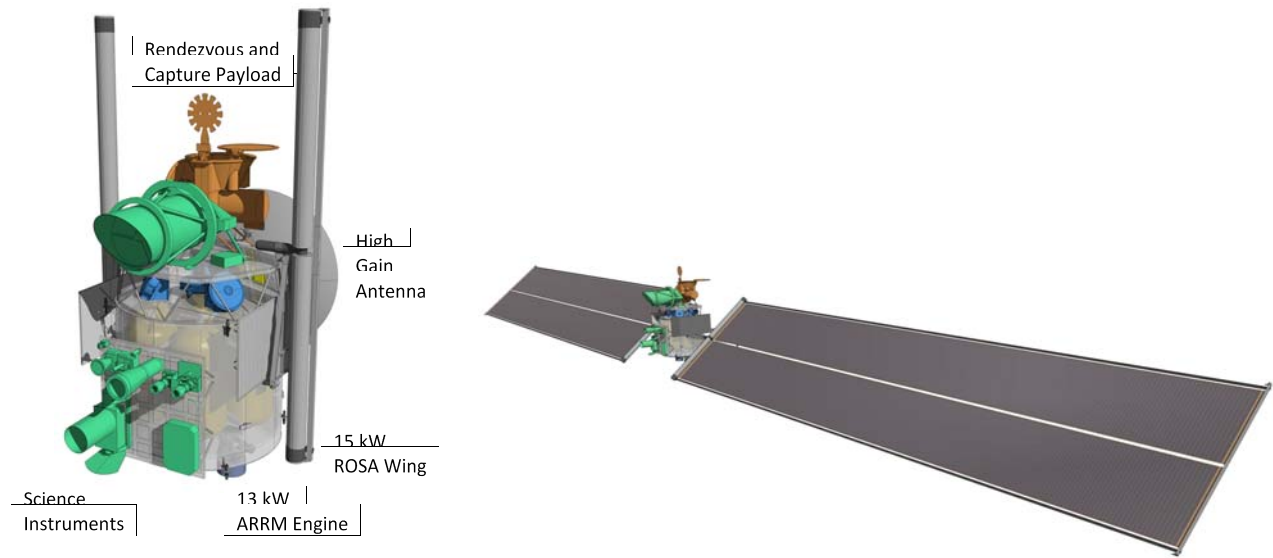


Fig. 7. Notional Mars Sample Return Orbiter spacecraft in stowed (left) and deployed (right) configurations.

to hold them) and the ΔV by 900 m/s (for the 15° plane change). This would yield a total mass of over 5100 kg, which exceeds the capability of the heaviest Atlas V class launch vehicles, and is over 50% heavier than the equivalent SEP mission.

An example of an orbiter configuration resulting from this analysis is shown in Fig. 7. The spacecraft stowed dimensions would be approximately 2.6 m in diameter and 4.8 m in height. This would easily fit in the fairing of an Atlas V-401 or Falcon 9 class launch vehicle. The deployed solar arrays would have a total surface area of 125 m² and provide 27 kW at Earth distance, and 10 kW at Mars aphelion. Although the ROSA array is depicted in this figure, both the ROSA and MegaFlex concepts are attractive and are being actively studied.

3. STARSHADE EXOPLANET MISSIONS

ARRM system performance is next examined for a trio of exoplanet observation mission concepts, where a starshade spacecraft must be repositioned frequently to observe different star targets.

Background

A starshade is a large deployable space structure that blocks starlight so that a companion space telescope can image orbiting exoplanets. It consists of a central disc and flower-like petals, as shown in Fig. 8, that are precisely shaped to control light diffraction. The science goal is to detect Earthlike exoplanets (exo-Earths) in habitable zones around Sun-like stars and, ultimately, to characterize them via spectroscopy to look for atmospheric biomarker gases. A specific goal for a compelling science mission is to detect at least ten exo-Earths.

Key starshade performance requirements are to suppress starlight by at least ten orders of magnitude (i.e. Earth

contrast at 1AU and quadrature illumination) and to operate at a small inner working angle (IWA, defined as the angle between the telescope boresight and the line connecting the telescope to the starshade tips), to access a sufficient number of habitable zones. For example, at 100-mas IWA the habitable zone is accessible at only a few dozen stars, but this grows to a few hundred stars at 50-mas IWA.

Small IWAs require large starshade-telescope separation distances. For example, a 50-mas IWA for the 40 to 60-m-dia. starshades considered here requires separation distances of 82 to 124-Mm. To line up on each new target star (i.e. retarget), the starshade must translate a large distance that is proportional to the separation distance. Retarget maneuver capacity is a critical performance metric and an efficient SEP system is required to provide the requisite capacity.

For launch, the starshade stows compactly around a central hub structure, as shown in Fig. 9, and is then deployed during the cruise from Earth to Earth-Sun-L2. Bus equipment including the SEP system hardware and propellant tanks are carried inside the central hub. SEP thrusters are mounted on the top and bottom decks of the hub; the opposing thrusters are used to accelerate and decelerate the starshade spacecraft during retargeting maneuvers. Fig. 10 shows a photo of prototype starshade hardware in the starshade development lab at JPL.

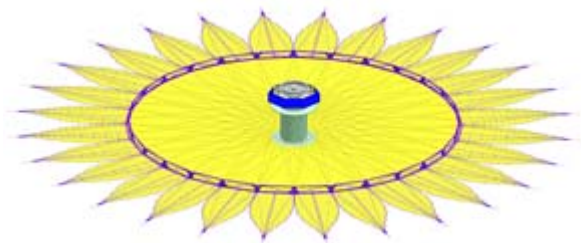


Fig. 8. Deployed Starshade.

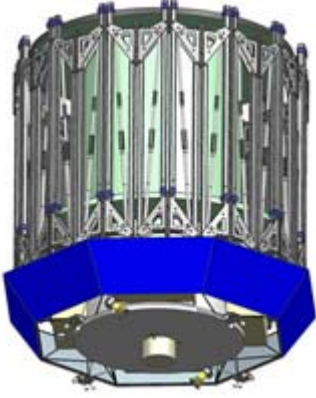


Fig. 9. Starshade Stowed Around Central Hub.



Fig. 10. Starshade prototype hardware at JPL. Stowed and deployed perimeter trusses in foreground and background. Petal on wall is 6-m long.

Study Approach and Mission Case Studies

Typically, starshade missions have targeted a variety of planet types and observed over a single, relatively wide bandpass (i.e., range of wavelengths) for both imaging (search mode) and spectroscopy (characterization). This represents a compromise in performance. A recent mission study took a different approach and demonstrated a dramatic increase in expected exo-Earth detections.¹⁷ First, all observations are focused on habitable zones. Second, an optimal combination of IWA, bandpass and target set is selected to maximize the total habitable zone search space, within the retarget capacity of available SEP systems. A reduced bandpass has the negative effect of increasing integration times, but this is balanced against the positive effect of reducing the IWA for greater habitable zone access.

The studies shown here utilize the new approach to optimize exo-Earth detections because it is more stressful for the SEP design. We evaluate the ARRM system performance for three science missions that are recommended by the Exoplanet Exploration Program Analysis Group (Exo-PAG) for study in the next decadal review.¹⁸ The companion telescope identifies these missions, as:

- Wide-Field Infrared Survey Telescope (WFIRST)
- Habitable-Exoplanet Imaging Mission (HabEx),
- Large UV/Optical/near-Infrared Surveyor (LUVOIR)

To be clear, WFIRST is a dark-energy mission that is already under study. The Exo-PAG recommendation is to study a separate Probe Class starshade mission to operate with and leverage WFIRST. In each mission case, the starshade launches separately to rendezvous with the telescope and conduct a 5-year exo-Earth search that uses less than 25% of telescope observing time. This is not meant to suggest that all missions would operate in this fashion, but this establishes a common metric.

The flight-proven BPT-4000 system is also considered in this study to both establish a technology fallback for the ARRM systems and to illustrate an interesting trade between thrust and specific impulse. Table 4 summarizes the salient parameters for both systems.

Table 4. SEP System Parameters Used for Starshade Mission Analysis.

Parameter	ARRM	BPT-4000
Thrust	526 mN	254 mN
Specific Impulse	3000 s	2020 s
PPU Input Power	13.3 kW	4.9 kW
Thruster Mass	43 kg	12.3 kg
PPU Mass	42 kg	12.5 kg
Thruster Dimension	52 cm dia.*	25 × 28 cm

* includes radiator plate

Mission Simulation Approach

A simplified mission simulation tool is used to support rapid and evolutionary parametric studies. It proves conservative relative to the more sophisticated starshade design reference mission (DRM) tool¹⁹ that takes hours to run each case. Key approximations for the simplified tool are that retarget motion is rectilinear and target stars are uniform in apparent distribution across the sky.

The starshade field of regard (FOR) is between 40 and 83° from the Sun. As the starshade and telescope orbit together around the Sun, candidate target stars pass through the FOR. The effect is that target stars must be selected to advance in ecliptic longitude at an average rate of 360° per year. An additional change in latitude is added at the rate of 20% of the longitude change, per DRM studies. This leads to an average retarget distance (s) as a function of the total number of retargets (N).

Using the rectilinear retargeting assumption, the low-thrust velocity profile consists of a linear acceleration (a), a long coast, and a linear deceleration. The time integral of velocity gives the applied translation distance as:

$$s = \frac{1}{4}at^2(2f - f^2) \quad (1)$$

where f is the fraction of total retarget time (t) that the thrusters are operating. We solve for f , compute the total retarget ΔV as:

$$\Delta V = N a f t \quad (2)$$

and compute the required propellant mass via the rocket equation. Dry mass is scaled from a reference mission with a 34-m-dia. starshade²⁰ and includes 30% contingency.

This formulation accounts for a low thrust penalty in ΔV that approaches a factor of two as f approaches unity. This is visually apparent as a triangular velocity profile with twice the height of the rectangular velocity profile of equal area, for the impulsive case. In practice, we limit f to not exceed 0.62, to avoid a runaway increase in propellant mass with small increase in the number of retargets N . The process is to incrementally increase the number of retargets at a given IWA until one of three constraints is reached:

- Launch wet mass = launch vehicle mass capacity
- Thruster fire time fraction (f) = 0.62
- Xenon volume = available central hub volume

This simplified mission simulation approach yields significantly higher ΔV requirements than matching runs of the DRM tool. This is likely because the DRM tool selects real stars from a catalog and their spatial distribution is very non-uniform. DRM retarget maneuvers are widely distributed in ΔV and low-thrust ΔV penalty. A significant fraction of the advance in target longitude occurs in efficient fashion as long coasts between clumps of targets. This suggests real potential for significant performance enhancement.

It must be noted, however, that this simplified approach has been compared to the DRM tool for only the WFIRST mission case, with relatively small separation distances. Larger separation distances for larger telescope missions may prove problematic as they approach a significant fraction of the halo orbit size. There is some concern that starshade observations may be restricted for some portion of each orbit and this remains to be studied. It is also noted that this concern does not apply to an Earth Drift Away orbit that may also be considered.

Power Generation for SEP

The main technology challenge for adding SEP to a starshade spacecraft is how to generate the large requisite power. Conventional solar arrays are problematic because they would cast solar shadows onto the starshade which would induce thermal deformations. The planned approach is to integrate solar cells into the optical shield portion of the starshade inner disc. The optical shield is an origami-folded structure of semi-rigid panels that deploys along with the perimeter ring truss. The panels are constructed of foam sandwiched between outer layers of 25- μm -thick black Kapton with rip-stop. The concept is to replace the Sun-facing layer of black Kapton for a subset of panels that are

populated with solar cells, as conceptually shown in Fig. 11. It is most critical to ensure that the added solar cells not interfere with the optical shield deployment kinematics.

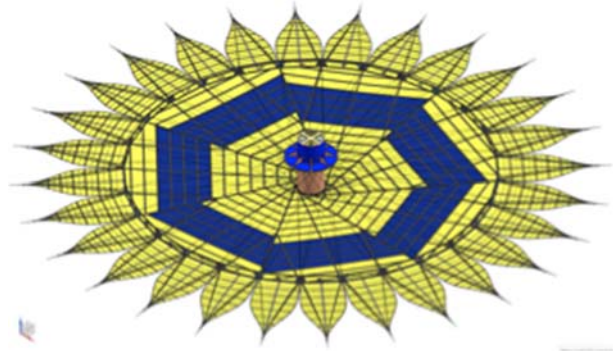


Fig. 11. Conceptual population of a subset of inner disc OS panels with thin film solar cells.

The baseline cell technology chosen here is amorphous silicon thin film photovoltaics with three chromatic junctions. The cells, coatings, and conductive traces are all vapor deposited onto a 25- μm -thick PV9103 Kapton substrate that is developed specifically for this purpose. The total thickness of added material is $\leq 1\text{-}\mu\text{m}$ and this is not expected to interfere with the optical shield deployment kinematics. Plans are in place to verify this with multiple “solar panel” prototypes integrated into an inner disc prototype. The expected end-of-life (EOL) conversion efficiency for this design is greater than 7%.²¹

The array is designed to account for all combinations of SEP power load and available inner disc area and follows the following rules:

- Solar incidence angle $\leq 40^\circ$
- Overall cell packing factor $\geq 75\%$
- System operating power margin $\geq 10\%$
- String loss $\leq 5\%$ and ohmic loss $\leq 2\%$

For the mission cases analyzed here, the cell efficiency required is between 5% and 7%. Hence, the low efficiency but very thin amorphous silicon cells appear to be a good match for this application.

The starshade with integrated solar array does not deploy immediately after launch, hence the spacecraft carries a separate body-mounted conventional solar array to provide electrical power for the bus. The starshade array is dedicated to SEP operations.

WFIRST Mission Case Study

The starshade designed to operate with the 2.4-m-dia. WFIRST telescope is 40-m in total diameter, with a 24-m-dia. inner disc and 8-m long petals. It launches on a Falcon 9 with 3700 kg mass capacity to Earth-Sun-L2. The average on-target time is 3.4 days. One ARRM thruster fires at a time for a SEP power demand of 13 kW. A cold spare in each direction brings the total number of thrusters to four and they

are cross-strapped to two PPU's. The volume available inside the spacecraft hub limits the xenon mass to 1680 kg, as computed for an integer number of commercially-available pressure vessels with a capacity of 210 kg each.

Fig. 13 shows the retarget capacity as a function of IWA for the WFIRST case. Retarget capacity for the ARRM system is launch-mass limited to 150 targets at the 52-mas IWA goal. The power equivalent BPT-4000 system case fires three thrusters at a time and has a total of eight thrusters, including one spare for each direction of motion. Retarget capacity for the BPT-4000 system is launch-mass limited to 139, only eleven fewer retargets, at the 52-mas IWA goal. Bipropellant thruster performance, shown for comparison, does not meet the minimum scientific goals.

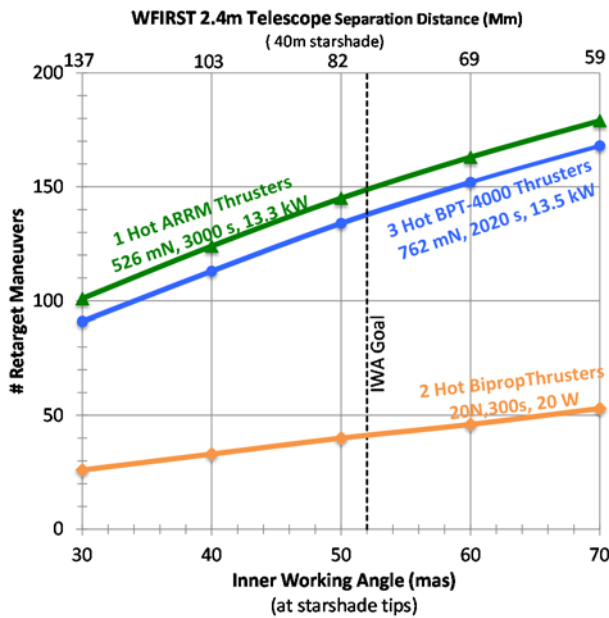


Fig. 13. WFIRST-Starshade Retarget Capacity.

The BPT-4000 system retarget capacity is surprisingly close to the ARRM system, even though the ARRM system has 50% higher specific impulse. There are two main reasons for this result. First, the higher total thrust of three BPT-4000 thrusters compared to one ARRM thruster suffers less of a low thrust ΔV penalty and reduces the ΔV by 19%. Second, a lower SEP dry mass for the BPT-4000 system means an extra 90 kg of xenon can be used.

HabEx Mission Case

The starshade designed to operate with the 4-m-dia. HabEx telescope is 48-m in total diameter, with a 30-m-dia. inner disc and 9-m long petals. It launches on an Atlas 551 with 6500 kg mass capacity to Earth-Sun L2. The average on-target time is 20 hours. Two ARRM thrusters fire at a time for total power demand of 27 kW. A cold spare in each direction brings the total number of thrusters to six and they are cross-strapped to three PPU's. The volume available inside the hub limits xenon mass to approximately 2500 kg.

Fig. 12 shows retarget capacity as a function of IWA for the HabEx case. Retarget capacity for the ARRM system is xenon-volume limited to 208 at the 40-mas IWA goal. The roughly power-equivalent BPT-4000 case fires six thrusters at a time. In this case no spares are carried, but rather a graceful degradation in performance is accepted. Retarget capacity for the BPT-4000 system is xenon-volume limited to 172 at the 40-mas IWA goal.

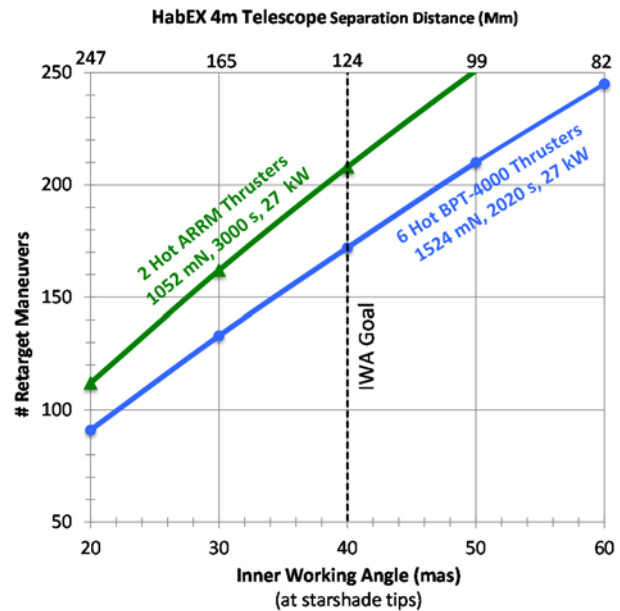


Fig. 12. HabEx-Starshade Retarget Capacity.

The BPT-4000 system has a similar advantage in thrust as in the WFIRST case, but the difference in SEP dry mass is much less and it does not translate into additional useable xenon, as both systems are limited to the same amount. This favors the ARRM system, but hinges on a rough estimate of available volume that requires further study.

LUVOIR Mission Case

The starshade specified to operate with the 10-m-dia. LUVOIR telescope is 60-m in total diameter, with a 36-m-dia. inner disc and 12-m long petals. The average on-target time is also 20 hours despite the larger aperture, due to operational overheads. The stowed starshade diameter exceeds the limit for 5-m-dia. launch fairings. The LUVOIR telescope also exceeds the 5-m-dia. fairing limit and the tentative plan is to launch on SLS. Given an early limit on SLS launches, this may not be an option to launch the starshade. Alternative vehicles might be future variants of the Delta IVH or Falcon 9H that may offer fairings larger than 5-m-dia. The launch mass capacity of this hypothetical launch vehicle is, of course, unknown. Here we identify the required launch mass capacity that matches a retarget capacity that is limited by other factors.

Three ARRM thrusters fire at a time for a total power demand of 40 kW. A cold spare in each direction brings the total number of thrusters to eight and they are cross-strapped to four PPUs. The hub diameter and height grow compared to the other telescope mission cases to carry up to 6200 kg of xenon.

Fig. 15 shows the retarget capacity as a function of IWA for the LUVOIR case. Retarget capacity is thruster-fire-time limited to 165 at the 35-mas IWA goal. Total estimated launch wet mass is 9200 kg, with 30% contingency. This seems like a reasonable launch capacity, but this is speculative. By comparison, the Delta IVH capacity to Earth-Sun-L2 with a 5-m-dia. fairing is 20,000 kg.

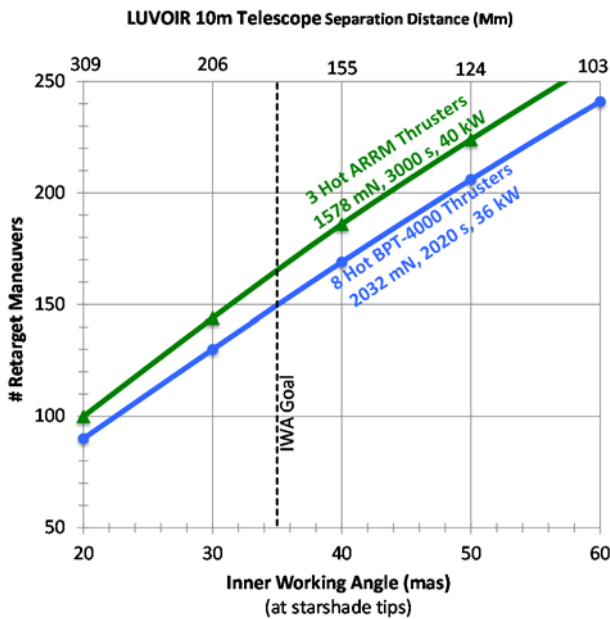


Fig. 15. LOUVIOR-Starshade Retarget Capacity.

The roughly power equivalent BPT-4000 case fires eight thrusters at a time. In this case no spares are carried, but rather a graceful degradation in performance is accepted. Retarget capacity for the BPT-4000 is xenon volume limited to 150, only fifteen fewer retargets, at the 35-mas IWA goal. However, an additional 1600 kg of xenon is required to perform this mission. This brings the total launch wet mass estimate to 11,000 kg, with 30% dry mass contingency. Although a significant amount of xenon is required for this mission case, the throughput per thruster is only 388 kg, within qualification limits.

Starshade Analysis Summary

The ARRM system retarget capacity detailed above is fed into a mission simulation tool that finds optimal combinations of IWA, bandpass and target set, with integration times. Fig. 14 shows the results for all three mission cases in terms of the cumulative habitable zone space searched. Multiplying this number by the frequency of exo-Earths gives the expected number of exo-Earth detections. All of the mission cases satisfy a goal to detect at least 10

exo-Earths, if the frequency of exo-Earths is $\geq 20\%$, which is a moderate value.²⁰

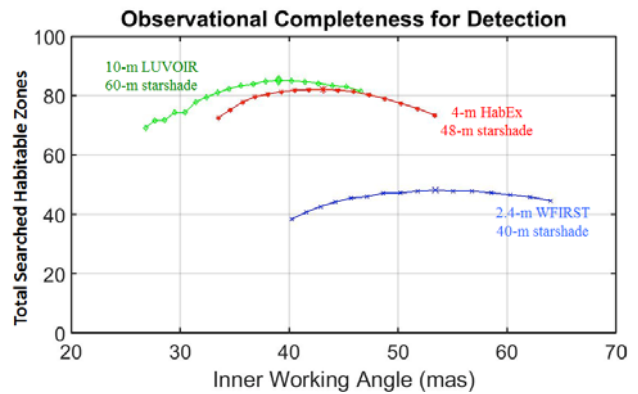


Fig. 14. Total Habital Zone Coverage Results.

The increasing starshade mass and retarget distances that go along with the larger telescope missions is accommodated by adding ARRM thruster strings. The BPT-4000 system is also shown to be a viable candidate. In each case, xenon throughput required for the mission is within the qualified lifetime. A more rigorous SEP and power system trade study is warranted, however, for these missions. The WFIRST, HabEx and LUVOIR missions retarget, respectively, with 1, 2 and 3 simultaneously-fired ARRM thrusters. The available solar array area grows at an almost proportional rate to the increasing power demand. All three-mission cases appear to be a good match for the baseline amorphous silicon thin film cells.

4. SUMMARY

High-power SEP technology developed by NASA's Space Technology Mission Directorate, a key technology for the Asteroid Redirect Robotic Mission (ARRM) concept, has generated excitement within NASA for other types of potential missions as well. Advantages for Mars orbiter missions are numerous: round-trip missions, large plane changes, improved payload accommodation, more flexible operations, etc. One specific case study demonstrated the delivery of 270 kg of payload to Mars orbit, followed by a 15° plane change, an orbital rendezvous with a sample cache, and a return trip to Earth, all on a Falcon 9 launch vehicle with a 27 kW solar array. This is a significant capability increase over chemically-propelled missions like the Mars Reconnaissance Orbiter. The benefits of the ARRM ion propulsion system also extend to starshade missions, where SEP is an enabling technology for the ambitious science goals of exo-planet observations. This system is shown to meet goals for detection of 10 exo-Earths, and also delivers greater science return than the state-of-the-art BPT-4000 Hall thruster system.

ACKNOWLEDGEMENTS

A portion of the work described in this paper was carried out by the Jet Propulsion Laboratory, California Institute of

Technology, under a contract with the National Aeronautics and Space Administration. Thanks to Scott Howe of JPL for producing the Mars Orbiter spacecraft configuration images.

REFERENCES

To be placed here...

BIOGRAPHY



Steve Snyder holds a B.S. in Aerospace Engineering from the University of Illinois and an M.S. and Ph.D. in Mechanical Engineering from Colorado State University. He has over twenty years of experience and fifty publications in the field of electric propulsion including research and development, formulation, systems

engineering, and flight implementation. He is presently the Lead Systems Engineer for the ARRM Ion Propulsion System. He has been the Lead Electric Propulsion Engineer for JPL's Team X, was a systems engineer for the Dawn Ion Propulsion System, and prior to joining JPL led major contributions to Space Systems/Loral's first satellites with electric propulsion systems.



David Manzella received a B.S. in Engineering from the University of Notre Dame in 1985, and M.S. in Engineering from the University of Toledo, and a Ph.D. in Engineering from Stanford University in 2005. He has worked at the NASA Glenn Research Center for more than 28 years. He is the chief engineer for the Solar

Electric Propulsion Technology Demonstration Project. He was previously a senior propulsion engineer responsible for research and development of on-orbit plasma propulsion components and systems with more than 75 technical publications on electric propulsion technology and mission applications.



Doug Lisman hopefully knows how to write a good bio. He received a B.S. in Engineering from California State University, Los Angeles in 1970. He has been with JPL for more than 25 years. He has been the study lead for MSR in the Mars Exploration Program Office at JPL. Prior to MSR, he supervised a systems

engineering group for JPL's projects implemented in partnership with industry. He has also managed systems engineering groups for instrument and payload development and has been involved in the formulation and development of numerous planetary and Earth-orbiting spacecraft and payloads. His career started with systems integration on the Apollo program for North American Rockwell.



Rob Lock received his B.S. degree in Mechanical Engineering from Cal Poly, San Luis Obispo in 1985. He has been with JPL for more than 27 years. He currently leads orbiter mission formulation studies for the Mars Exploration Program Office at JPL. He has been Mission Manager for the JPL payloads on the ExoMars Trace Gas Orbiter mission, lead mission planner for Mars Reconnaissance Orbiter mission and mission planning team chief for the Magellan Mission to Venus. He was the lead systems engineer for the Jupiter Europa Orbiter mission study and has led systems engineering, operations design, and aerobraking design for Mars Scout proposals. His career started with work on ISS, Strategic Defense Initiative, and Magellan spacecraft development at Martin Marietta Aerospace in Denver Colorado.



Austin Nicholas received a B.S. degree in Aerospace Engineering from University of Illinois at Urbana-Champaign in 2011. He received an S.M. in Aeronautics and Astronautics from the Massachusetts Institute of Technology in 2013. He currently works for JPL in the Project Systems Engineering & Formulation Section. His primary focus is developing concepts for various Mars missions, including Mars Sample Return. At MIT, he worked on attitude and cluster control for a formation-flight Cubesat mission using electrospray propulsion and architecture exploration for low-cost human missions to the lunar surface.



Ryan Woolley received a B.S. in Physics-Astronomy from Brigham Young University in 2003, a M.S. in Astronautical Engineering from USC in 2005, and a Ph.D. in Aerospace Engineering from the University of Colorado in 2010. He has been with JPL since 2005. Ryan began his tenure as a systems engineer in the Mars Mission Concepts group and has since transferred to the Inner Planets Mission Design group. He has worked on nearly all aspects of the Mars Sample Return campaign and has developed various tools to evaluate mission designs and architectures. He is currently working on the Next Mars Orbiter specializing in low-thrust mission design.

1. Sovey, J.S., V.K. Rawlin, and M.J. Patterson, "Ion Propulsion Development Projects in the U.S.: Space Electric Rocket Test 1 to Deep Space 1," *Journal of Propulsion and Power*, 2001. 17(3): p. 517-526.
2. NASA Research Announcement, *Game Changing Opportunities in Technology Development*. Solicitation NNL12A3001N, Appendix B, 2012; Available from: <http://nspires.nasaprs.com/external/viewrepositorydocument/cmdocumentid=319936/solicitationId=%7B66840A2F-0937-3BD2-9811-5F4FC1B2830A%7D/viewSolicitationDocument=1/SAS%20APPENDIX%20B%20Final.pdf> [Cited Oct. 9, 2015].
3. NASA Press Release, *Here Comes the Sun: NASA Picks Solar Array System Development Proposals*, Release 12-270, Aug. 10, 2012, http://www.nasa.gov/home/hqnews/2012/aug/HQ_12-270_Solar_Array_Selections.html, [Cited Oct. 9, 2015].
4. Mikellides, I.G., I. Katz, R.R. Hofer, D.M. Goebel, K. De Grys, and A. Mathers, "Magnetic Shielding of the Acceleration Channel Walls in a Long-Life Hall Thruster," AIAA 2010-6942, 46th Joint Propulsion Conference, Nashville, TN, July 25-28, 2010.
5. Hofer, R.R., D.M. Goebel, I.G. Mikellides, and I. Katz, "Design of a Laboratory Hall Thruster with Magnetically Shielded Channel Walls, Phase II: Experiments," AIAA 2012-3788, 48th Joint Propulsion Conference, Atlanta, GA, July 30 - Aug. 1, 2012.
6. Mikellides, I.G., I. Katz, R.R. Hofer, and D.M. Goebel, "Design of a Laboratory Hall Thruster with Magnetically Shielded Channel Walls, Phase III: Comparison of Theory with Experiment," AIAA 2012-3789, 48th Joint Propulsion Conference, Atlanta, GA, July 30 - Aug. 1, 2012.
7. Hofer, R.R., H. Kamhawi, D.A. Herman, J.E. Polk, J.S. Snyder, I.G. Mikellides, W. Huang, J. Myers, J. Yim, G. Williams, A. Lopez Ortega, B.A. Jorns, M. Sekerak, C. Griffiths, R. Shastry, T.W. Haag, T. Verhey, B. Gilliam, I. Katz, D.M. Goebel, J.R. Anderson, J. Gilland, and L. Clayman, "Development Approach and Status of the 12.5 kW HERMeS Hall Thruster for the Solar Electric Propulsion Technology Demonstration Mission," IEPC 2015-186, 34th International Electric Propulsion Conference, Kobe, Hyogo, Japan, July 4-10, 2015.
8. Kamhawi, H., W. Huang, T.W. Haag, R. Shastry, R. Thomas, J. Yim, D.A. Herman, G. Williams, J. Myers, R.R. Hofer, I.G. Mikellides, M. Sekerak, and J.E. Polk, "Performance and Facility Background Pressure Characterization Tests of NASA's 12.5-kW Hall Effect Rocket with Magnetic Shielding Thruster," IEPC 2015-007, 34th International Electric Propulsion Conference, Hyogo, Kobe, Japan, July 4-10, 2015.
9. Herman, D.A., W. Santiago, H. Kamhawi, J.E. Polk, J.S. Snyder, R.R. Hofer, and J.M. Parker, "The Ion Propulsion System for the Solar Electric Propulsion Technology Demonstration Mission," IEPC 2015-008, 34th International Electric Propulsion Conference, Hyogo-Kobe, Japan, July 4-10, 2015.
10. Pinero, L.R., K.E. Bozak, W. Santiago, R.J. Scheidegger, and A.J. Birchenough, "Development of High-Power Hall Thruster Power Processing Units at NASA GRC," AIAA 2015-3921, 51st Joint Propulsion Conference, Orlando, FL, July 27-29, 2015.
11. NASA Solicitation, *Thruster and Power Processing Unit Development for an Advanced Electric Propulsion System*. Solicitation NNC15ZCH014R, 2015; [Cited Oct. 9, 2015].
12. Mazanek, D., R.G. Merrill, J.R. Brophy, and R. Mueller, "Asteroid Redirect Mission Concept: A Bold Approach for Utilizing Space Resources," IAC-14,D3,1,8,x25965, 65th International Astronautical Congress, Toronto, Canada, Sept. 29 - Oct. 3, 2014.
13. Mattingly, R. and L. May, "Mars Sample Return as a Campaign," 2011 IEEE Aerospace Conference, Big Sky, MT, Mar. 5-12, 2011. DOI: 10.1109/AERO.2011.5747287.
14. Oh, D.Y. and D. Landau, "A Simple Semi-Analytic Model for Optimum Specific Impulse Interplanetary Low Thrust Trajectories," IEPC 2011-010, 32nd International Electric Propulsion Conference, Wiesbaden, Germany, Sept. 11-15, 2011.
15. Woolley, R.C. and A.K. Nicholas, "SEP Mission Design Space for Mars Orbiters," AAS 15-632,

- AAS/AIAA Astrodynamics Specialist Conference, Vail, CO, Aug. 9-13, 2015.
16. Lock, R.E., Z.J. Bailey, T.D. Kowalkowski, E.L. Nilsen, and R.L. Mattingly, "Mars Sample Return Orbiter Concepts Using Solar Electric Propulsion for the Post-Mars2020 Decade," 2014 IEEE Aerospace Conference, Big Sky, MT, Mar. 1-8, 2014. DOI: 10.1109/AERO.2014.6836477.
 17. Seager, S., M. Turnbull, W. Sparks, M. Thomson, S.B. Shaklan, A. Roberge, M. Kuchner, N.J. Kasdin, S. Domagal-Goldman, W. Cash, K. Warfield, D. Lisman, D. Scharf, D. Webb, R. Trabert, S. Martin, E. Cady, and C. Heneghan, "The Exo-S Probe Class Starshade Mission," in *Proceedings of the 2015 SPIE Conference*, San Diego, CA, 2015.
 18. *Exoplanet Exploration Program Analysis Group (ExoPAG) Report to Paul Hertz Regarding Large Mission Concepts to Study for the 2020 Decadal Survey (Oct. 6, 2015)*. 2015; Available from: https://exep.jpl.nasa.gov/files/exep/ExoPAG_Large_Missions.pdf [Cited Oct. 19, 2015].
 19. Trabert, R., S. Shaklan, P.D. Lisman, A. Roberge, M. Turnbull, S. Domagal-Goldman, and C. Stark, "Design Reference Missions for the Exoplanet Starshade (Exo-S) Probe-Class Study," in *Proceedings of the 2015 SPIE Conference*, San Diego, CA, 2015.
 20. *Exo-S: Starshade Probe-Class Exoplanet Direct Imaging Mission Concept, Final Report (March 2015)*. 2015; Available from: http://exep.jpl.nasa.gov/stdt/Exo-S_Starshade_Probe_Class_Final_Report_150312_URS250118.pdf [Cited Oct. 19, 2015].
 21. Personal Communication, Wilt, D., AFRL, Oct. 2015.